Geophys. J. Int. (2008) **173,** 932–941 doi: 10.1111/j.1365-246X.2008.03770.x

Space–time correlation of earthquakes

Patrizia Tosi,[1] Valerio De Rubeis,[1] Vittorio Loreto[2] and Luciano Pietronero[2]

[1] *Istituto Nazionale di Geofisica e Vulcanologia, Roma, Italy. E-mail: tosi@ingv.it*
[2] *'La Sapienza' University, Physics Department, and INFM, Center for Statistical Mechanics and Complexity, Roma, Italy*

Accepted 2008 February 25. Received 2008 February 25; in original form 2005 July 4

SUMMARY

Seismicity is a complex process featuring non-trivial space–time correlations in which several forms of scale invariance have been identified. A frequently used method to detect scale-invariant features is the correlation integral, which leads to the definition of a correlation dimension separately in space and time. In this paper, we generalize this method with the definition of a space–time combined correlation integral. This approach allows us to analyse medium-strong seismicity as a point process, without any distinction among main, after or background shocks. The analyses performed on the catalogue of worldwide seismicity and the corresponding reshuffled version strongly suggest that earthquakes of medium-large magnitude are time clustered inside specific space–time regions. On the basis of this feature, we recognize a space–time domain statistically characterized by sequences' behaviour and a domain of temporal randomness. Then, focusing on the spatial distribution of hypocentres, we find another domain confined to short distances and characterized by a relatively high degree of spatial correlation. This spatial domain slowly increases with time: we interpret this as the 'afterevent' zone representing the set of all subsequent events located very near (about 30 km) to each reference earthquake and embedded on specific seismogenic structures such as faults planes.

Key words: Persistence, memory, correlation, clustering; Fractals and multifractals; Earthquake interaction, forecasting, and prediction; Statistical seismology.

1 INTRODUCTION

Seismogenic sources demonstrate their resistance limit to stress loading with the generation of earthquakes; stress is redistributed to neighbouring areas, causing the aftershock sequence to develop in space and in time. Stress is probably redistributed because a sequence occurrence brings the medium to a new dynamic equilibrium. This interpretation requires clarification of several issues; one of them is the triggering of earthquakes. Short-range triggering (at a distance of the order of seismic source dimension) may be sufficiently justified by stress changes induced by the main shock. Long-range triggering is a more controversial topic, with arguments of both physical and statistical nature. Experimentally, some authors have recognized long-range triggering in real data (Hill *et al.* 1993), most cases come from geothermal sites (Husen *et al.* 2004), but there are examples even in non-volcanic areas (Brodsky *et al.* 2000). Godano *et al.* (1999) have shown, through a statistical approach, that for a seismic de-clustered catalogue to reach a complete Poissonian behaviour, it is not sufficient to remove only seismic events close in space after a main event, but it is necessary to exclude long-distance short-time seismic activity too. Others have proposed physical explanations, including Coulomb-stress modifications (King *et al.* 1994; Stein *et al.* 1994; Stein 1999; Melini *et al.* 2002; Marzocchi *et al.* 2003) and multiple stress transfer (Ziv 2006). Statistically, an interesting class of models has been proposed invoking, for example, a cellular-automata-like behaviour of the crust, considered in a critical state (Bak & Tang 1989). Earthquakes are the dynamic outcome of a very complex system whose critical properties are accessible through the observation of the existence of scaling relations. Dynamic critical phenomena are very well studied in physics: from the seminal review of Hohenberg & Halperin (1977), a long literature has been developed, showing the existence of time-correlation functions for critical point systems. The advantage of assuming a critical state is that, at long distances, a trigger effect can be obtained by a relatively small amount of stress: rupture is achieved by a pre-existent load on a fault surface plus a relatively small portion of far away produced stress, sufficient to cause the event. This new event can itself produce a new stress redistribution and so on. This chain of stress–strain transfer can introduce an interesting component of the system considered as a whole: a relation between space and time, both in short- and long-range earthquake interactions. Several authors have attempted to find space–time influence ranges after big main shocks in specific regions and in worldwide catalogues. Influence regions of the order of 100 km from main shocks are likely to occur (e.g. Gasperini & Mulargia 1989; Reasenberg 1999). Interestingly, for the largest earthquake of last century, Lomnitz (1996) found very long-range correlation and a gap around 300 km, partly explained with a directional effect due to source geometry. Huc & Main (2003) and Marsan & Bean (2003) addressed the issue of stress diffusion at global level. They found that the mean triggering distance increases with time very slowly compared with a normal diffusion process. They did not

make any *a priori* assumption about the role of each event, considering every earthquake-–regardless of its magnitude—as a possible triggering event of the following seismicity. Marsan *et al.* (2000) investigated space–time relations of scale-invariance of seismicity in three seismic catalogues differing in space and time ranges. They pointed out that space and time should not be considered separately, but rather the spatial correlation structure is evolving in time. This implies migration of aftershocks away from the main shock. It takes the form of a power-law growth with a small diffusion exponent indicating a subdiffusive process.

Despite the wide interest and the richness of interpretations stimulated by these topics, there are still open issues. Should long-range triggering be considered to be a normal process, or rather it is a rare occurrence limited to particular conditions (for example, the presence of fluids)? Is there a limit of the influence area of an event? Does it depend on the magnitude and elapsed time? Is the traditional division of seismicity into main, after and background real or only necessary for a better comprehension of the phenomenon? To address these questions, it is important to consider the spatial and temporal aspects of the seismic process simultaneously, in a combined way. In this work we apply a novel method of analysis (Tosi *et al.* 2004), suitable to point processes and based on space–time correlations among earthquakes. Like the previously cited authors, we do not separate seismicity into main and aftershocks. We consider medium-high energy global seismicity where every event can be considered a potential main shock.

2 SCALE-INVARIANCE IN GLOBAL SEISMICITY

In the time domain, a main shock is usually followed by aftershocks with a decay rate described by the Omori law (Utsu *et al.* 1995). This law, considering either its original version or its nested development incorporated into the ETAS model (Ogata 1988), produces a clustering of seismicity. For specific regions, the time clustering has been evidenced through the fractal dimension of earthquake occurrences (Smalley *et al.* 1987; De Rubeis *et al.* 1997). Moreover, there are evidences that clustering is varying over time, resulting in a multifractal distribution of earthquakes (Godano & Caruso 1995).

Space distribution of seismicity on a large scale follows the most significant tectonic structures such as plate limits, large fault systems and volcanic complexes. Nevertheless, inside these preferred regions, seismicity cannot be fully characterized by a defined distribution. The concept of background seismicity has been postulated in addition to sequence evolution, with the intention to better fit all possible temporal and spatial behaviours. Despite all these efforts, space location of seismicity remains problematic; for these reason new approaches, such as scale invariance, have been investigated. Quantification of this feature is possible through the definition of the spatial fractal dimension of epicentres (Kagan & Knopoff 1980). Very different values have been measured for different times in specific areas (De Rubeis *et al.* 1993). Thus, for example, in Central Italy, the background seismicity is recognized to have a rather high spatial fractal dimension whereas shortly before and during sequences, it displays much lower values (Tosi 1998). Other authors have noted that spatial scale invariance is not homogeneous and therefore a multifractal character has been evidenced (Hirata & Imoto 1991; Hirabayashi *et al.* 1992; Dimitriu *et al.* 2000).

A frequently used method to analyse scale-invariance in seismicity is the correlation integral (Grassberger & Procaccia 1983). It is defined as.

$$C(l) = \frac{2}{N(N-1)} \sum_{i=1}^{N-1} \sum_{j=i+1}^{N} \Theta(l - \|\mathbf{x}_i - \mathbf{x}_j\|), \tag{1}$$

where l is the metric of the space considered, N is the total number of elements, $\mathbf{x}$ is the coordinate vector and Θ is the Heaviside step function. If (1) scales like a power law, $C(l) \propto l^D$, the correlation dimension D can be defined by

$$d(l) = \frac{\delta \log C(l)}{\delta \log l},\ D = \lim_{l \to 0} d(l). \tag{2}$$

Experimentally, self-similarity can best be found by plotting the local slope d of $\log C(l)$ versus $\log l$ (Kantz & Schreiber 1997).

We searched for self-similarity in global seismicity by using the National Earthquake Information Center (USGS) catalogue for the time period 1973–2004, with magnitudes $M_b \geq 5.0$. This catalogue selection was conditioned by completeness criteria and it consists of events with a magnitude distribution from medium to high.

The correlation integral applied to the earthquake occurrence time t,

$$C(\tau) = \frac{2}{N(N-1)} \sum_{i=1}^{N-1} \sum_{j=i+1}^{N} \Theta(\tau - \|t_i - t_j\|) \tag{3}$$

is shown in Fig. 1 both on bi-logarithmic and local-slope plots. The result is a very stable behaviour lasting over almost all the scales investigated. The correlation dimension D (eq. 2) is well defined. With least-square fit on the log–log plot in the time range 24 min to 3000 d we obtain $D = 0.94$, a value very close to the embedding dimension ($D = 1$)—this means that, on a global scale, the temporal distribution of seismicity can be considered to be very nearly random.

The correlation integral applied to the earthquake spatial distribution

$$C(r) = \frac{2}{N(N-1)} \sum_{i=1}^{N-1} \sum_{j=i+1}^{N} \Theta(r - \|\mathbf{x}_i - \mathbf{x}_j\|), \tag{4}$$

where $\mathbf{x}$ is the space coordinate vector, is shown in Fig. 2. Distances between hypocentres are measured in 3-D space and connecting points with the shortest straight line—this implies that two hypocentres localized at two antipodal points on the earth's surface are separated by a distance equivalent to the earth's diameter. For space, a quite different behaviour is evident. For shorter ranges (from 3 to 30 km), the least-square fit reveals a high correlation dimension ($D = 1.95$); this value progressively decreases, reaching $D = 1.20$ for distances over 300 km. The error affecting the hypocentral localization can increase the true dimension; nevertheless, the value corresponding to short distances is far from the one of the embedding space ($D = 3$), pointing rather at the value proper of a smooth surface, probably the fault planes. The low dimension for long distances reflects the fact that global seismicity falls on plate boundaries, which are linear on such a scale.

3 SPACE–TIME COMBINED CORRELATION INTEGRAL

We know that seismicity is dominated by sequences that are clustered in time and space, but this behaviour does not appear to leave fingerprints in correlation integral analysis at a global scale (Figs 1 and 2). The reason has to be found in the fact that, in the calculation of $C(\tau)$, earthquake pairs are counted regardless of their spatial distances. In the same manner, in the calculation of $C(r)$,

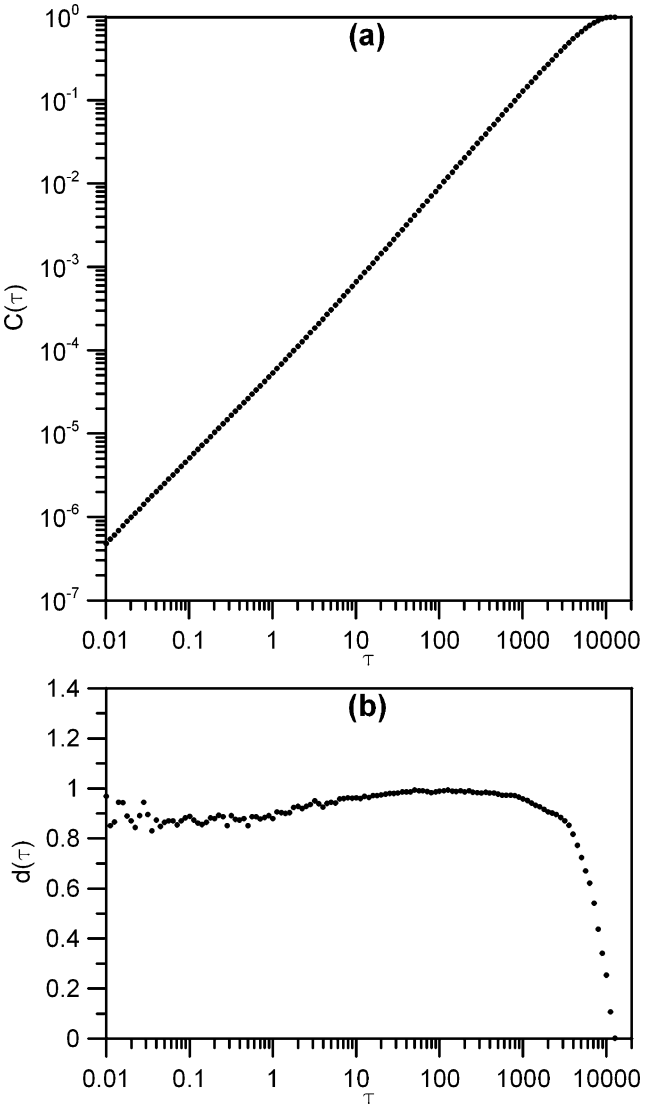

Figure 1. (a) Correlation integral of global seismicity in time. Intertime τ is expressed in days. (b) Local slopes of (a).

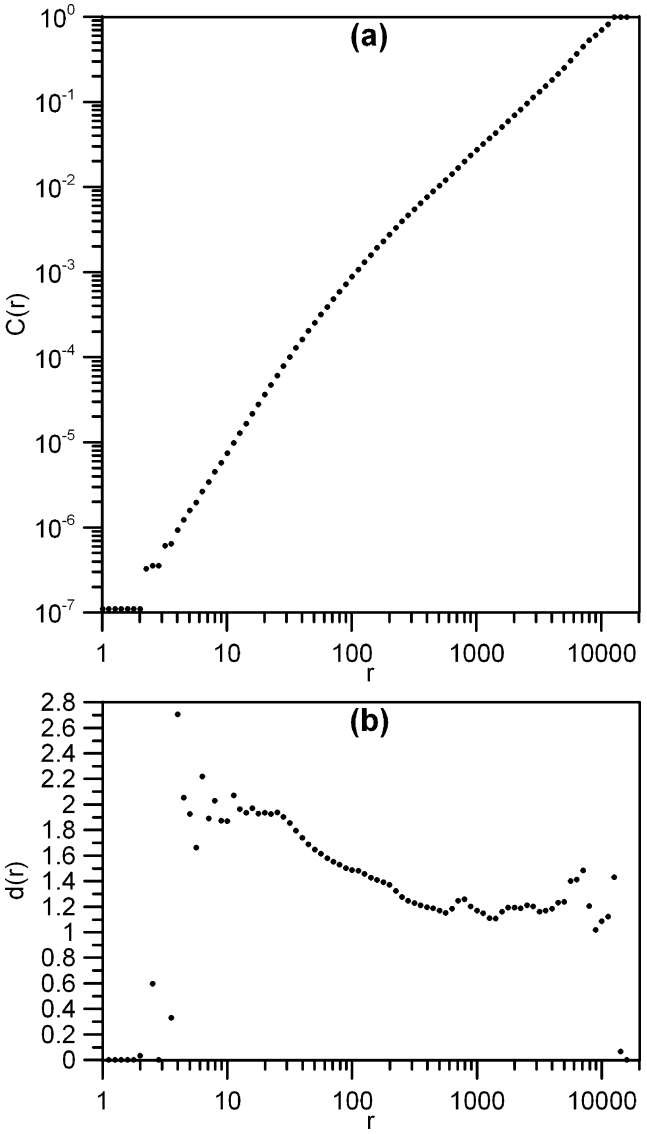

Figure 2. (a) Correlation integral of global seismicity in space: r is the distance in km between hypocentres. (b) Local slopes of (a).

earthquake pairs are counted regardless of their time separation. Seismicity is a phenomenon acting simultaneously in space and time, and any attempt to separate these two aspects may result in too drastic simplifications. It is with this spirit that we introduce here a new approach leading to a self-consistent analysis of both spatial and temporal correlations. We define the space–time combined correlation integral as follows.

$$C_c(r,\tau) = \frac{2}{N(N-1)} \sum_{i=1}^{N-1} \sum_{j=i+1}^{N} [\Theta(r - \|\mathbf{x}_i - \mathbf{x}_j\|) \cdot \Theta(\tau - \|t_i - t_j\|)]. \quad (5)$$

This general definition include eq. (3) when $r = r_{\max}$ and eq. (4) when $\tau = \tau_{\max}$. This generalization of the correlation integral can be applied to every phenomenon described by a set of dimensions with not comparable measurement units. The application to seismicity calls for a simultaneous analysis of four coordinates: three spatial and one temporal. As a consequence, it will be possible to calculate interdistances among events in both space and time units. The combined correlation integral representation is no longer a 2-D plot as for eqs (1), (3) and (4), but is a surface plot (Fig. 3). Actually for any data set having no connection between time and space, $C_c(r, \tau)$, for each r and τ, is the product of the respective correlation integrals that, in this case, can be viewed as the probability to find pairs up to that value of r and τ.

$$C_c(r,\tau) = C(r) \cdot C(\tau). \quad (6)$$

Similarly to eq. (2), we define the time correlation dimension D_t and its local slope d_t as

$$d_t(r,\tau) = \frac{\partial \log C_c(r,\tau)}{\partial \log \tau}, \; D_t(\tau) = \lim_{\tau \to 0} d_t(r,\tau), \quad (7)$$

and the space correlation dimension D_s with its local slope d_s as

$$d_s(r,\tau) = \frac{\partial \log C_c(r,\tau)}{\partial \log r}, \; D_s(r) = \lim_{r \to 0} d_s(r,\tau). \quad (8)$$

Under the hypothesis of events distributed randomly and without any connection between space and time, both d_t and d_s would be constant for all r and τ, equal to the respective embedding dimension values. Under the different hypothesis of events with two

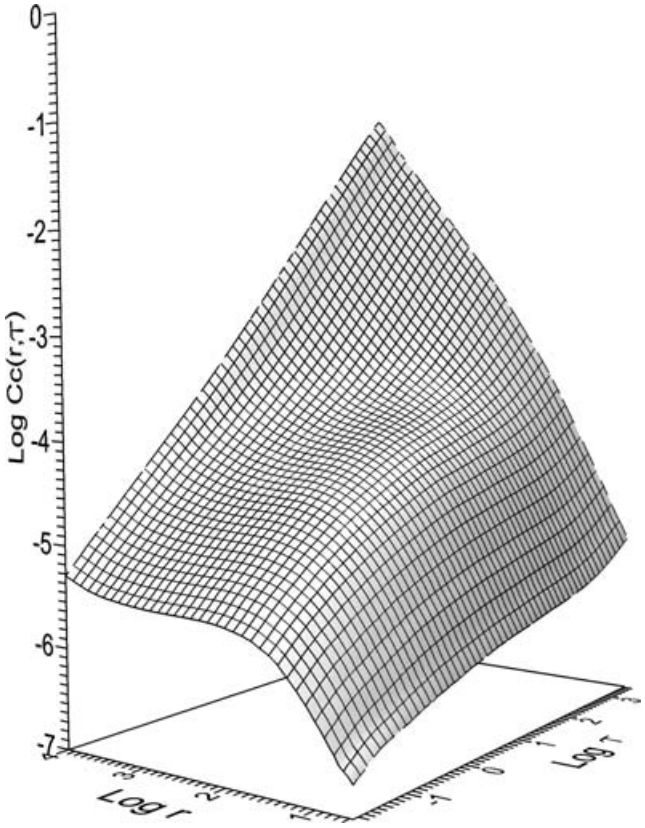

Figure 3. Space–time combined correlation integral C_c (r, τ). For r equal to the maximum distance in the catalogue, the C_c surface reduces to the plot in Fig. 1(a), whereas for τ equal to the whole time data span, C_c reduced to the plot in Fig. 2(a).

independent space and time power-law total distributions, d_t would be equal to the total D_t for all r and d_s, equal to the total D_s for all τ.

4 TIME CORRELATION DIMENSION

The correlation dimension varies between 0 and the value of the embedding dimension, which for time is 1. Moreover, the correlation dimension is a direct measure of clustering: having a set of points with the correlation dimension equal to the embedding space means that this set covers it completely. Conversely, a set with low correlation dimension reveals clustering and, at limit, d_t $(r, \tau) = 0$ means that all elements of the set are concentrated at a point (which has the topological dimension equal to 0). The correlation dimension is also related with the randomness content of the set. From statistics we know that a random process occupies all the space available, resulting in a statistically complete and homogeneous covering of the embedding space.

In Fig. 4, we show the local slope of time correlation dimension d_t (eq. 7) for global seismicity data as a function of time interval τ and hypocentral distance r. Values are represented only when the number of non-cumulated pairs, in the corresponding space–time bin, is greater than five. One clear time clustering domain appears, with d_t less than 0.5. On the contrary, for long time intervals and large interdistances, the time correlation dimension is close to one, indicating random occurrence. The time clustering is limited at relatively small distances: this is an evidence of local time correlation, typical of the sequence structures. The boundary between clustering and random character is not located on a line with a constant r, but its setting is function of space and time intervals among earthquakes. The patterns observed in Fig. 4 significantly support the hypothesis

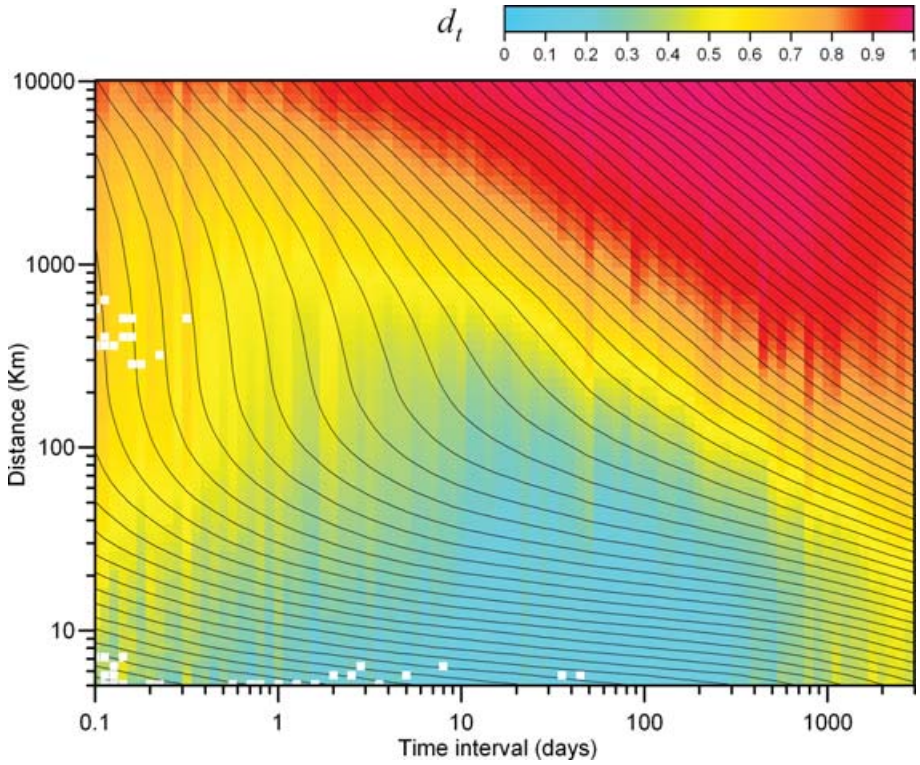

Figure 4. Local slopes of time correlation dimension d_t (r, τ) (in colour; white squares correspond to insufficient earthquake couple number) for global seismicity. Dark contour lines represent the space–time combined correlation integral C_c (r, τ).

that earthquakes, inside specific space–time domains, do not behave randomly, hence showing clustering (low d_t values).

To check the validity of this experimental result, we applied the same analysis to the global catalogue after a reshuffling procedure. Reshuffling consists in randomly mixing the time occurrences of all events maintaining their hypocentral coordinates. This procedure safeguards the statistical properties of data separately for time and space, but it destroys the mutual connections. The result shows (Fig. 5) that all patterns vanish, evidencing constant high values of d_t at all distances and time intervals. The experimental result of the reshuffling procedure closely confirms the theoretical prediction (eq. 6). Under the assumption of the complete absence of any mutual correlations between space and time, d_t values at distances less than maximum distance are only the result of a random undersampling, hence identical to d_t of the total distribution (Fig. 1). The not-coloured area on left-hand side down corner of Fig. 5, reflects the absence of a minimum amount of earthquake pairs (fixed, as in Fig. 4, to five non-cumulated pairs) necessary to a reliable calculation of $C_c\ (r, \tau)$. In fact, the reshuffling procedure has lowered the probability of finding two earthquakes near in space and close in time.

The radical difference between d_t calculated on real and reshuffled data demands further interpretation of the clustering domain. The transition from low to high d_t is not abrupt and poses the question of how to set a separation limit. To this purpose, we produced a random global catalogue with the same number of events as the real one, but with randomly distributed time and space occurrence. For space we considered a uniform distribution of points on a sphere with random depth in the range 0–700 km. For time we assigned to each event a random occurrence inside the time span of the catalogue. As expected, all d_t values are very near 1, with average $\overline{d_t} = 0.99$ and standard deviation $\sigma = 0.10$. Since approximately 98 per cent of all data have $d_t \geq 0.8$, it is reasonable to assume this value as a threshold value above which the catalogue is characterized by random time occurrences.

The limit value $d_t = 0.8$ also separates approximately 98 per cent of time correlation dimension data obtained with the reshuffled seismicity (Fig. 5). Thus we can state, with sufficient confidence, that all values $d_t > 0.8$ obtained with real seismicity (Fig. 4) represent a realization of a time random process with independent spatial and temporal occurrences. Note the very gradual transition from high to low d_t values determining the absence of a clear boundary. Our previous statistical test was able to discriminate the random domain, but there is no univocal, objective reference value to separate a clustering domain. We can indicate $d_t \leq 0.5$ as values corresponding to a sensible clustering and $0.5 < d_t < 0.8$ as a transition zone where the interpretation is more questionable. A detailed analysis of $d_t = 0.5$ boundary is shown in Fig. 6. In the time range 10–1000 d, the boundary decays as a power law: $r \propto \tau^{-\alpha}$ with $\alpha = 0.6$. The whole transition zone follows the same behaviour, confirming the general character of the decay. In fact, even for different d_t boundaries (0.4, 0.6 and 0.8), the power-law behaviour is maintained (Fig. 7).

It is important to analyse if there is a variation of the clustering domain in relation to the magnitude. To check this hypothesis, the magnitude of all *i*th events in the catalogue, referring to eq. (5) was limited, respectively, in the ranges 5.0–5.5, 5.5–6.0 and 6.0–6.5 while the *j*th events maintained the $M \geq 5.0$ catalogue threshold for all different tests. Note that *j*th events can have a larger magnitude than the respective band-limited *i*th event: the aim is to study the influence of each event on the subsequent ones. Results are shown in Fig. 7: increasing the magnitude, all three d_t boundaries (0.4, 0.6 and 0.8) migrate to greater distances. This result might be

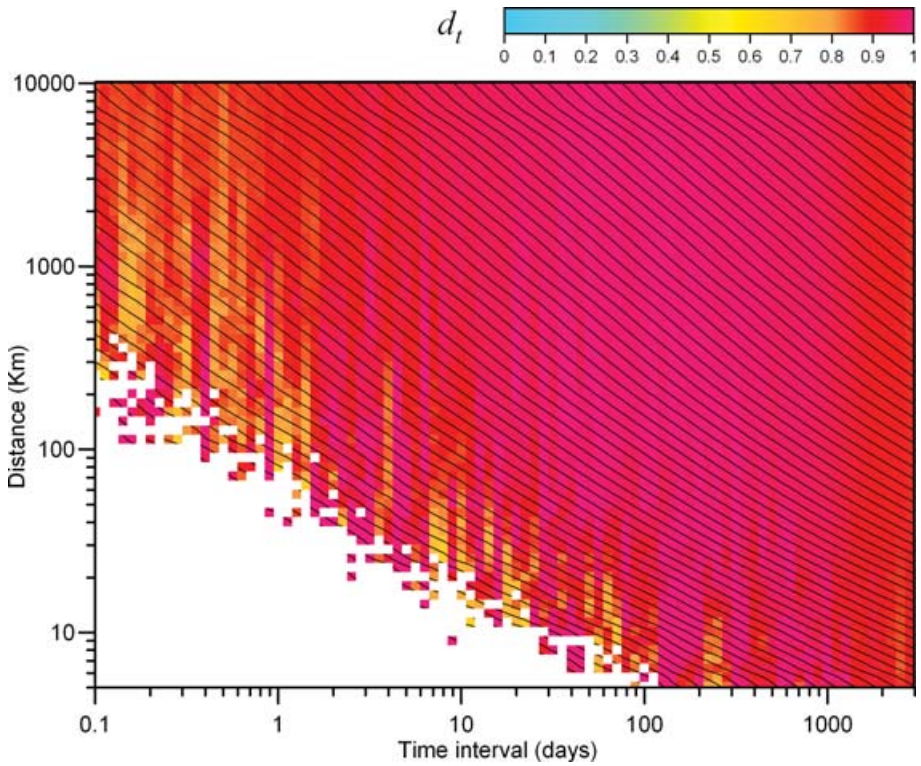

Figure 5. Local slopes of time correlation dimension $d_t\ (r, \tau)$ (in colour; white squares correspond to insufficient earthquake couple number) and space–time combined correlation integral $C_c\ (r, \tau)$ (dark contour lines) for reshuffled catalogue.

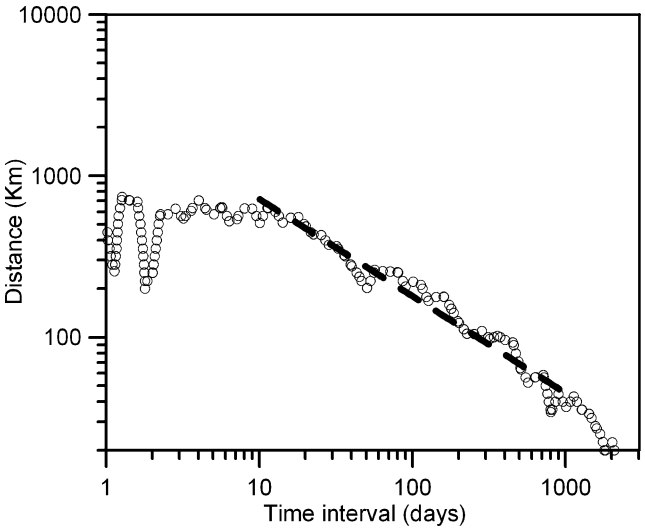

Figure 6. The value $d_t = 0.5$ has been chosen to represent the limit between time clustering (lower left-hand side) and time randomness (upper right-hand side, see Fig. 4). Dashed line is the linear fit in time range 10–1000 d.

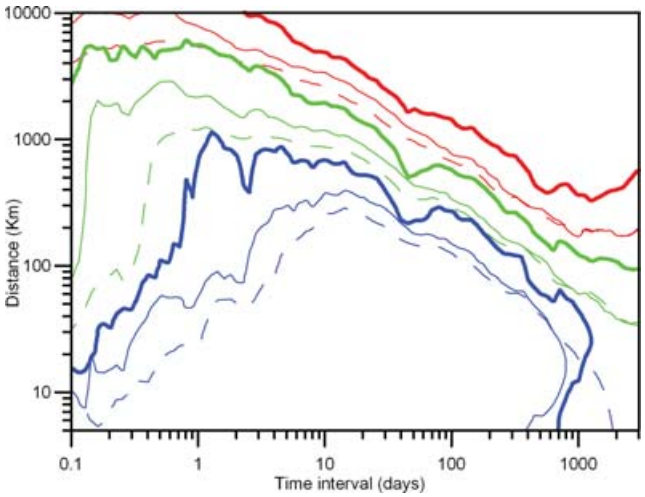

Figure 7. Space–time variation of some d_t limits as function of magnitude of the reference i event. The colours correspond to different d_t values: blue for $d_t = 0.4$, green for $d_t = 0.6$ and red for $d_t = 0.8$; line style denotes magnitude interval: dashed line, $5.0 \leq m_b < 5.5$; solid line $5.5 \leq m_b < 6.0$ and bold solid line, $6.0 \leq m_b < 6.5$.

influenced by the reduced number of i events in a higher magnitude range. To exclude this possibility, we repeated the analysis on the whole catalogue ($M \geq 5.0$) randomly, reducing the number of i events, matching in turn the number corresponding to the three magnitude classes. The resulting boundaries, displayed in Fig. 8, are coincident for the same d_t: it follows that earthquake number does not significantly influence the pattern. The enlargement of the time clustering domain in function of magnitude is probably linked with the changing proportion between the number of main and aftershocks with the increase of ith event magnitude.

To test further the general stability of the results with respect to the number of data, the global catalogue has been reduced to one tenth of the events randomly chosen (to reduce both i and j events). The d_t average of ten independent realizations is displayed in Fig. 9, showing that the result is very similar to that obtained using the whole data set (Fig. 4).

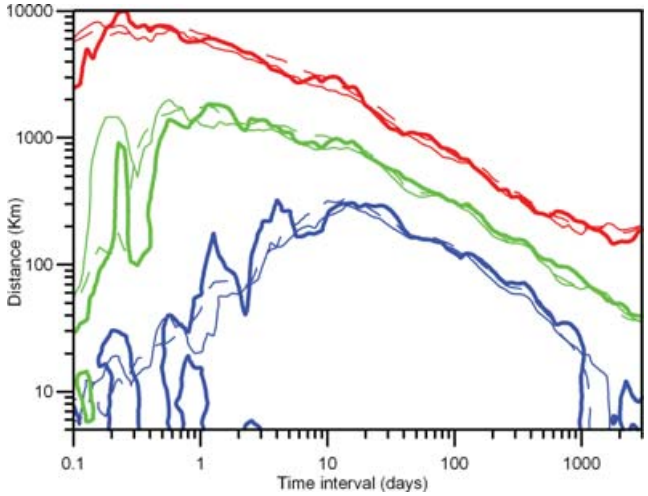

Figure 8. Space–time variation of the d_t limits shown in Fig. 7 after random reduction of the number of i events independently from the magnitude (line colours and styles as in Fig. 7).

The power law of the time clustering boundary appears to be a stable characteristic for a wide range of d_t values. From Figs 7 to 9, it results the permanence of the behaviour in the time span 10–1000 d with $\alpha \approx 0.6$. At very short time intervals, the clustering domain is more variable. Low d_t limits (0.4–0.5) show a trend opposite to the previous one, displaying an increasing of distance trough time. This suggests a peculiar influence of the sequence during the first day after the parent shock occurrence.

The real difference between results obtained with the combined correlation integral (eq. 7) and time fractal dimension as defined by eq. (2) is the highlighting of the temporal clustering behaviour at short interdistances. It is interesting to note that this clustering has variable limits over time, depicting an evolution probably related to the sequence generated by each event.

5 SPACE CORRELATION DIMENSION

The space correlation dimension d_s is obtained deriving the combined correlation integral C_c with respect to interdistances r (eq. 8). Its behaviour for global seismicity is shown in Fig. 10. The pattern of d_s is quite different from that of d_t (Fig. 4): this is no surprise because these are two completely different aspects of seismicity. The fact that both quantities vary as a function of space and time is due to the intrinsic complexity of the process. It appears evident that the pattern of d_s values is much more articulated than the simple spatial fractal dimension calculated following eq. (4). In fact, the resulting bi-valued behaviour (Fig. 2), evidenced by neglecting time intervals, is represented now as the particular endpoint case at the right-hand end of the plot in Fig. 10.

Dimension values, for this case, can range from 0 to 3, because hypocentres are embedded in a 3-D space. Actually d_s does not reach the value of 3 for two intrinsic reasons: first, global seismicity is depth limited, being forced by brittle rheology of the crust into the first few hundreds of kilometres: this dimension is small if compared with the whole latitude and longitude extension; second, seismicity tends to be located on planar features such as seismogenic faults, or linear patterns as plate boundaries. The effects of these geophysical factors result in lowering of hypocentre dimension, which is confined to a value lower than 2.2. Larger values

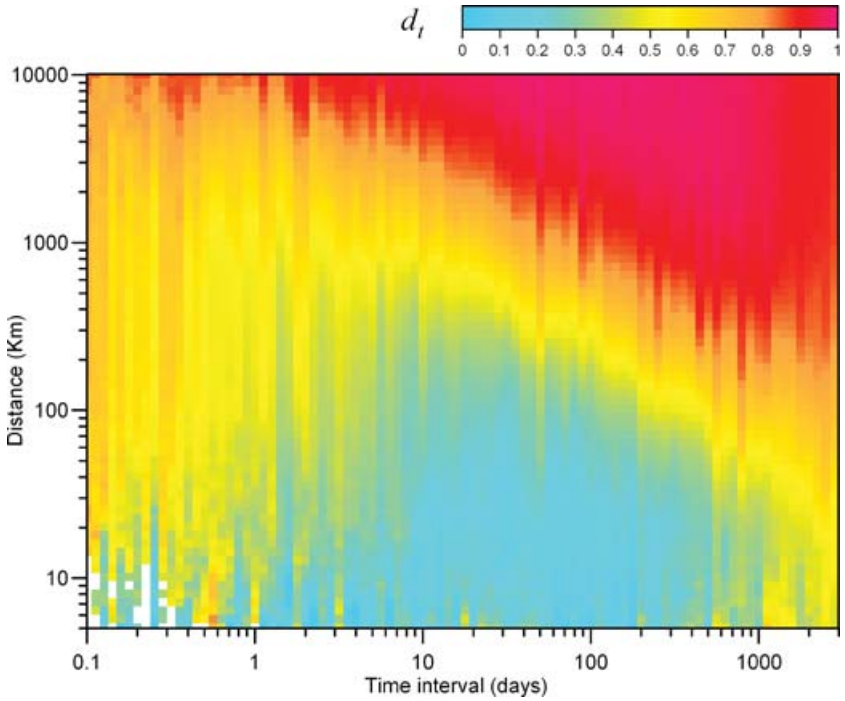

Figure 9. Mean d_t values obtained from 10 independent realization of a reduced seismic catalogue; for every realization 10 per cent of total data were retained.

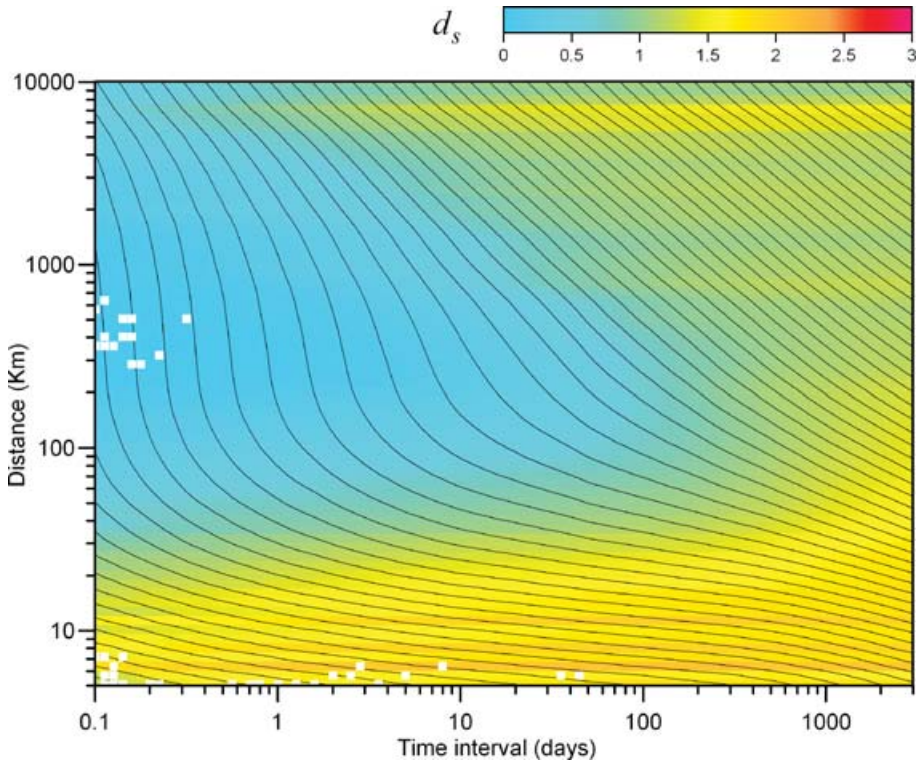

Figure 10. Local slopes of space correlation dimension d_s (r, τ) for global seismicity (in colour). Dark contour lines represent the space–time combined correlation integral C_c (r, τ). White squares correspond to a number of earthquake couples less then five.

($1.5 < d_s < 2$) in Fig. 10 are found at short interdistances (10–20 km); values near 2 indicate that hypocentres at this scale are embedded on simple surfaces. A large domain of $d_s < 1$ is located at bigger distances and time intervals less than 100 d. This is due to the low number of event couples inside this range (but higher than the necessary minimum amount to guarantee the calculation of d_s): inside this space–time domain, seismicity is not diffused, but is structured in isolated sequences. Within time intervals longer than 100 d, there is another domain of d_s values around 1, reflecting a distribution of points over linear structures.

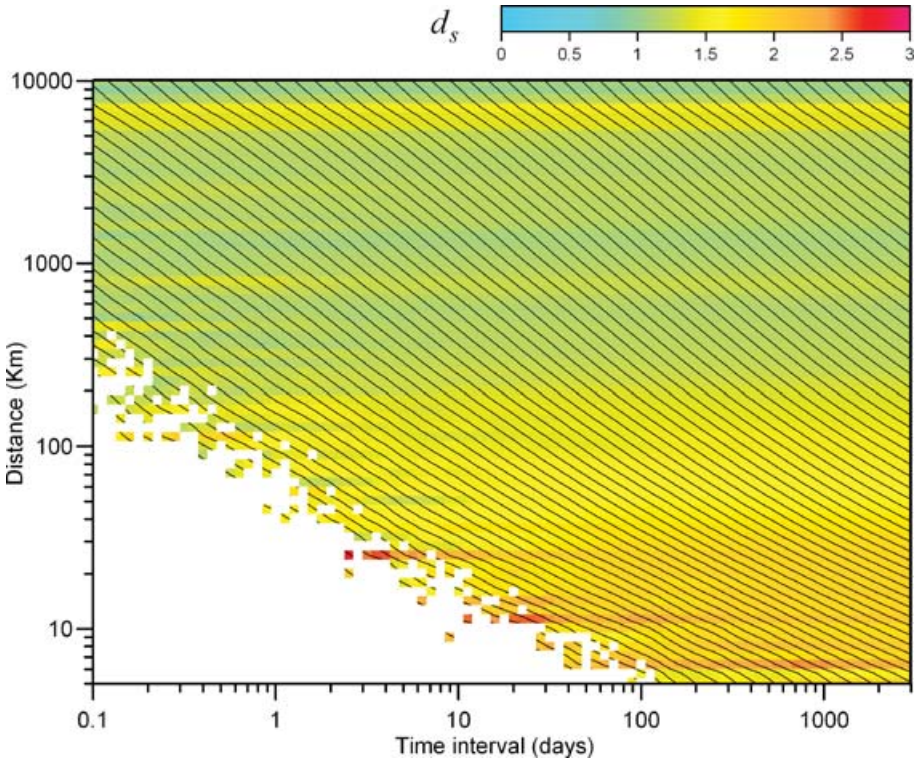

Figure 11. Local slopes of space correlation dimension d_s (r, τ) (in colour) and space–time combined correlation integral C_c (r, τ) (dark contour lines) for reshuffled catalogue. White squares correspond to a number of earthquake couples less then five.

The latter is placed prevalently on long distances and over long time intervals and is probably due to the presence of plate boundaries that, at these scales, can be approximated to simple lines.

Even in this case, we wanted to test the goodness of the results applying the same analysis on the reshuffled catalogue. The resulting plot (Fig. 11) shows that the non-combined statistical properties of data are not sufficient to produce the clustering domains, but a real connection between space and time is needed. Similarly to d_t behaviour of the reshuffled catalogue for which there was not difference of values at different distances, d_s has the same value for all time intervals, being nothing more that a random undersampling of the whole data set (Fig. 2).

Short interdistances in Fig. 10 are certainly influenced by localization error. In fact, it has been experimentally proven that noise increases the fractal dimension of a data set (Ben-Mizrachi *et al.* 1984). In case of sole influence of localization error, the limit of high d_s should be independent from intertime; but it clearly appears that, increasing the time interval, values of high d_s can be found up to greater distances, suggesting a physical process. For example, arbitrarily choosing $d_s = 1$ as the limit value between high d_s and space clustering (Fig. 12), a linear fit in the log–log plot describes well the power-law increase. Least-squares fit inside time interval 2.4 hr to 100 d is

$$\log r = 0.09 \log \tau + 1.5. \tag{9}$$

Consider that the importance of the result is not due to the specific values of coefficients but to the evidence of a specific relatively high valued d_s domain expanding in time; moreover, after choosing other threshold values ($0.7 \leq d_s \leq 1.3$), the resulting fit becomes very similar to eq. (9). As this d_s domain pertains to very short distances, we suppose that it is linked to the hypocentre distribution inside the seismogenic zone.

Over this border the low d_s domain gives a quantification of the clustering of the set of seismic zones.

Due to the presence of the localization error at these short distances and to the scarce reliability of high magnitude estimates, we chose to avoid to study the variation of eq. (9) in respect to the earthquake magnitude.

We have to stress that the way we followed to calculate hypocentral distances has a minimum influence on the results. In fact, using other distances definitions, as the simple surface epicentral distance (Tosi *et al.* 2004), all shown analyses give very similar outcome.

6 DISCUSSION

The introduction of the combined correlation integral (eq. 5) with its related d_s and d_t extends and completes the meaning of correlation integral applied separately in space and time to a distribution of seismic events. Figs 4 and 10 show that non-random patterns appear when space and time are analysed in a combined way. The results show a statistical property of the global seismicity of medium-high magnitude, which can be interpreted as an average behaviour of seismic events following each earthquake. Basically there are two different and independent domains, conceptually well separated: a domain of low d_t values, showing that time clustering spatially shrinks in time, and a domain of high d_s, acting at short distances and slowly expanding in time. Now we will discuss this behaviour in greater detail.

After the occurrence of an event, there is a space–time domain inside which the subsequent events are temporally clustered (Fig. 4). Inside this domain the seismic sequences drive temporal occurrences and their behaviour is still recognizable. High d_t values show that there are spatial distances and temporal intervals in which seismic occurrences result to be random. The reason lies in the temporal

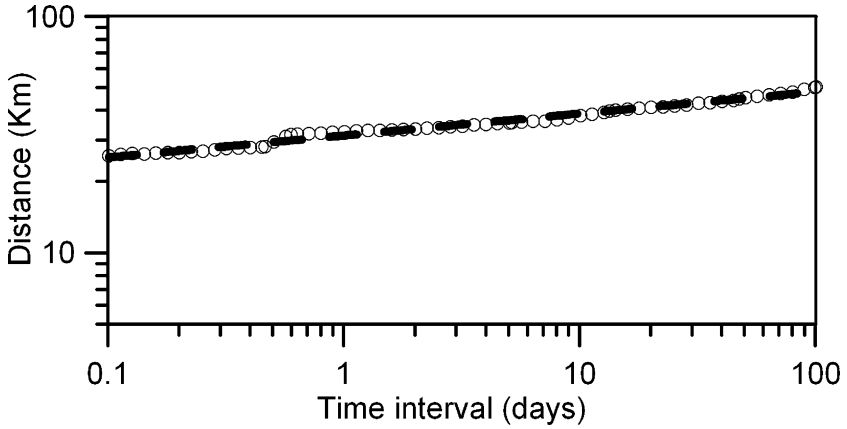

Figure 12. Time intervals τ and interdistances r for which $d_s = 1.0$, representing the limit between space clustering (upside) and higher values of d_s (downward, see Fig. 10) corresponding to dimension of a line up to that of a plane. In the time range from 2.4 hr to 100 d, least-square fit of points in log–log scale results in the line of equation $\log\ r = 0.09\ \log\ \tau + 1.5$.

overlapping of a sufficient number of independent sequences: this hides the underlying local time clustering.

The pattern of clustering sequences can be clearly delineated because our method shows an averaged behaviour of all possible sequences stacked together. Another reason is the low influence of background seismicity due to the high threshold magnitude of the catalogue. Our analysis indicates that the spatial limit of the temporal clustering domain increases with magnitude and shrinks over time following a power law (Fig. 7). This result clarifies the important role of the ranges considered in a seismic catalogue. Depending on the spatial or temporal extension of the catalogue, the statistics of the temporal occurrences will be different.

The results from the analysis of the space correlation dimension d_s reveals the presence of a space clustering of hypocentres for distances greater than 40 km and for time intervals less than 1 yr. For longer time intervals, the disappearance of spatial clustering reveals the seismic structures related to pre-existing tectonic settings, such as plate boundaries; after a sufficiently long time evolution, seismicity will tend to fill these seismic structures up to dimensions of thousands of kilometres. At short distances, d_s values mark clearly the presence of a zone, around each source, where hypocentres are not space clustered. The pairs of events, belonging to this domain, are characterized by time clustering, as all corresponding r and τ are below the limit depicted in Fig. 6. Events occurring in the 3 months after a reference earthquake within distances of 20–40 km from it are probably located on the same fault plane or in its immediate vicinity. We call them 'afterevents' following Marsan *et al.* (1999) because, in our approach, any earthquake (of magnitude greater than 5) can be the reference one, not only the main shock. From Fig. 12 it results that the size of the 'afterevent' zone slowly increases with time, following the relation (9). The limit $d_s = 1$ chosen may appear arbitrary, but changing it around this value gives fitting relations very similar to (9). The exponent of the corresponding power law ($r \propto \tau^{0.1}$) is very low: this allows for the possibility that data could be equally well fitted with a logarithmic relation. Several authors, using different methods, have noted an expansion of the aftershock area. Tajima & Kanamori (1985) evidenced a general increase of the area bounded by fixed threshold levels of seismic energy flux after a main shock, noting that in some cases this expansion is very slow. Recently Helmstetter *et al.* (2003) found a very weak diffusion of seismic activity in recognized sequences. Different approaches where used by Marsan *et al.* (2000), Marsan & Bean (2003), Huc & Main (2003) and McKernon & Main (2005). All of them considered the behaviour of all earthquake pairs. In particular, Marsan *et al.* (2000) and Marsan & Bean (2003) focused on the diffusion of time-correlated events normalized with the mean activity considered as background. Huc & Main (2003) corrected mean distances of seismic events using a reshuffled catalogue, whereas McKernon & Main (2005) involved in the normalization process of both the increasing surface area and event distances from a random catalogue. All of them describe the migration by a law of the form $\bar{d}(t) \propto t^H$, where $\overline{d}(t)$ is the mean distance between the main event and aftershocks occurring after time t, with an exponent $H < 0.5$ corresponding to a subdiffusive process. Godano & Pingue (2005) obtained similar results by measuring the increase of the spatial jump dividing each earthquake pair compared with their time interval. Despite the extreme difference among methods applied in the cited papers and our approach—which evaluates time variations of a short range area of homogeneous value of d_s and does not consider the rate or the probability of aftershocks occurrence—it is interesting to note that, inside the same time intervals and spatial ranges, there is the increase of an area following the same general law with exponent H of the same order.

7 CONCLUSIONS

With the introduction of the combined method of analysis, we extend and complete the information given by the correlation integral analysis as applied to seismicity. Interesting behaviours can be evidenced while they remained otherwise hidden when their space and timescale invariance were analysed separately. The results of our analysis show clearly specific seismicity patterns. In fact, all events concurred to the same result after having performed a sort of stacking procedure. The main result regarding time evolution is the statistical characterization of seismic activity. The apparent disagreement between the random time behaviour showed by correlation integral analysis applied to the global catalogue and the clear existence of seismic sequences is clarified by the results of the space–time combined analysis. The random character stems from the superimposition of several sequences over a sufficiently large area. In fact in a large area seismicity saturates time dimension giving, as result, a homogeneous random behaviour. This implies

the great influence of spatial extension and time span of a seismic catalogue on its statistical properties.

Concerning spatial domain, it is worth to note a space clustering for distances longer than 20–40 km. An inner zone of non-clustered 'afterevents', probably connected to the same seismogenic structure, is slowly increasing in time, in agreement with subdiffusion evidenced by several authors.

Variations of the limiting distances of clustering behaviour and 'afterevent' zones are indicated, respectively, by the general experimental relations $r \propto \tau^{-\alpha}$ and $r \propto \tau^{\beta}$ (eq. 9). Specific distance values are dependent on the magnitude of the reference event and on the (partly arbitrary) choice of limiting values of d_t and d_s. This work is intended to give statistical indications of the intertwining between space and time dynamics of global seismicity.

ACKNOWLEDGMENTS

This paper is dedicated to the memory of Petros Dimitriu who provided helpful advices for the first draft of this work. The authors thank I. Main for his constructive criticism and C. Godano for useful discussing. The National Earthquake Information Center, U.S.G.S., is acknowledged for the use of the earthquake catalogue.

REFERENCES

Bak, P. & Tang C., 1989. Earthquakes as a self-organized critical phenomenon, *J. geophys. Res.,* **94,** 15 635–15 637.

Ben-Mizrachi, A., Procaccia, I. & Grassberger, P., 1984. The characterization of experimental (noisy) strange attractors, *Phys. Rev. A,* **29,** 975–977.

Brodsky, E. E., Karakostas, V. & Kanamori, H., 2000. A new observation of dynamically triggered regional seismicity: earthquakes in Greece following the August, 1999 Izmit, Turkey earthquake, *Geophys. Res. Lett.* **27,** 2741–2744.

De Rubeis, V., Dimitriu, P., Papadimitriu, E. & Tosi, P., 1993. Recurrent patterns in the spatial behaviour of Italian seismicity revealed by the fractal approach, *Geophys. Res. Lett.,* **20,** 1911–1914.

De Rubeis, V., Tosi, P. & Vinciguerra, S., 1997. Time clustering properties of seismicity in the Etna region between 1874 and 1913, *Geophys. Res. Lett.,* **24,** 2331–2334.

Dimitriu, P.P., Scordilis, E.M. & Karacostas, V.G., 2000. Multifractal analysis of the Arnea, Greece seismicity with potential implications for earthquake prediction, *Nat. Hazards,* **21,** 277–295.

Gasperini, P. & Mulargia, F., 1989. A statistical analysis of seismicity in Italy: the clustering properties, *Bull. seism. Soc. Am.,* **79,** 973–988.

Godano, C. & Caruso, V., 1995. Multifractal analysis of earthquake catalogues, *Geophys. J. Int.,* **121,** 385–392.

Godano, C. & Pingue, F., 2005. Multiscaling in earthquakes diffusion, *Geophys. Res. Lett.,* **32,** L18302.

Godano, C., Tosi, P., De Rubeis, V. & Augliera, P., 1999. Scaling properties of the spatio-temporal distribution of earthquakes: a multifractal approach applied to a Californian catalogue, *Geophys. J. Int.,* **136,** 99–108.

Grassberger, P. & Procaccia, I., 1983. Measuring the strangeness of strange attractors. *Physica D,* **9,** 189–208.

Helmstetter, A., Ouillon, G. & Sornette, D., 2003. Are aftershocks of large Californian earthquakes diffusing? *J. geophys. Res.,* **108,** 2483–2506.

Hill, D.P. *et al.*, 1993. Seismicity remotely triggered by the magnitude 7.3 Landers, California, earthquake, *Science,* **260,** 1617–1623.

Hirabayashi, T., Ito, K. & Yoshii, T., 1992. Multifractal analysis of Earthquakes, *Pure appl. Geophys.,* **138,** 591–610.

Hirata, T. & Imoto, M., 1991. Multi-fractal analysis of spatial distribution of microearthquakes in the Kanto Region, *Geophys. J. Int.,* **107,** 155–162.

Hohenberg, P.C. & Halperin, B. I., 1977. Theory of dynamic critical phenomena, *Rev. Mod. Phys.,* **49,** 435–479.

Huc, M. & Main, I.G., 2003. Anomalous stress diffusion in earthquake triggering: correlation length, time dependence, and directionality, *J. geophys. Res.,* **108,** 2324–2335.

Husen, S., Wiemer, S. & Smith, R.B., 2004. Remotely triggered seismicity in the Yellowstone National Park region by the 2002 M_w 7.9 Denali Fault earthquake, Alaska, *Bull. seism. Soc. Am.,* **94**(6B), 317–331.

Kagan, Y. Y. & Knopoff, L., 1980. Spatial distribution of earthquakes: the twopoint correlation function, *Geophys. J. R. astr. Soc.,* **62,** 303–320.

Kantz, H. & Schreiber, T., 1997. *Nonlinear Time Series Analysis,* Cambridge University Press, Cambridge.

King, G.C.P., Stein, R.S. & Lin, J., 1994. Static stress changes and the triggering of earthquakes, *Bull. seism. Soc. Am.,* **84,** 935–953.

Lomnitz, C., 1996. Search of a worldwide catalog for earthquakes triggered at intermediate distances, *Bull. seism. Soc. Am.,* **86,** 293–298.

Marsan, D. & Bean, C., 2003. Seismicity response to stress perturbations, analysed for a world-wide catalogue, *Geophys. J. Int.,* **154,** 179–195.

Marsan, D., Bean, C.J., Steacy, S. & McCloskey, J., 1999. Spatio-temporal analysis of stress diffusion in a mined-induced seismicity system, *Geophys. Res. Lett.,* **26,** 3697–3700.

Marsan, D., Bean, C.J., Steacy, S. & McCloskey, J., 2000. Observation of diffusion processes in earthquake populations and implications for the predictability of seismicity systems, *J. geophys. Res.,* **105,** 28 081–28 094.

Marzocchi, W., Selva, J., Piersanti, A. & Boschi, E., 2003. On the long-term interaction among earthquakes: some insight from a model simulation, *J. geophys. Res.,* **108,** 2538–2550.

McKernon, C. & Main, I.G., 2005. Regional variations in the diffusion of triggered seismicity, *J. geophys. Res.,* **110,** B05S05.

Melini, D., Casarotti, E., Piersanti, A. & Boschi, E., 2002. New insights on long distance fault interaction, *Earth planet. Sci. Lett.,* **204,** 363–372.

Ogata, Y., 1988. Statistical models for earthquake occurrence and residual analysis for point processes, *J. Am. Stat. Assoc.,* **83,** 9–27.

Reasenberg, P.A., 1999. Foreshock occurrence before large earthquakes, *J. geophys. Res.,* **104,** 4755–4768.

Smalley, R.F. Jr., Chatelain, J.L., Turcotte, D.L. & Prévot, R., 1987. A fractal approach to the clustering of earthquakes: applications to the seismicity of the New Hebrides, *Bull. seism. Soc. Am.,* **77,** 1368–1381.

Stein, R. S., 1999. The role of stress transfer in earthquake occurrence, *Nature,* **402,** 605–609.

Stein, R. S., King, G.C.P. & Lin, J., 1994. Stress triggering of the 1994 M = 6.7 Northridge, California, earthquake by its predecessors, *Science,* **265,** 1432–1435.

Tajima, F. & Kanamori, H., 1985. Global survey of aftershock area expansion patterns, *Phys. Earth planet. Inter.,* **40,** 77–134.

Tosi, P., 1998. Seismogenic structure behavior revealed by spatial clustering of seismicity in the Umbria-Marche region (Central Italy), *Annali di Geofisica,* **41,** 215–224.

Tosi P., De Rubeis V., Loreto, V. & Pietronero, L., 2004. Space-time combined correlation integral and earthquake interactions, *Ann. Geophys.,* **47,** 1849–1854.

Utsu, T., Ogata, Y., & Matsu'ura, S., 1995. The centenary of the Omori formula for a decay law of aftershock activity, *J. Phys. Earth,* **43,** 1–33.

Ziv, A., 2006. What controls the spatial distribution of remote aftershocks? *Bull. seism. Soc. Am.,* **96**(6) 2231–2241.